



**Host Institution:**  
**PETRU PONI Institute of Macromolecular Chemistry of  
Romanian Academy**  
41-A, Grigore Ghica Voda Alley, 700487 Iași, Romania

**Contracting Authority:**  
**Executive Unit for Financing Higher Education  
Research Development and Innovation,**  
Romania

## **EXPLORATORY RESEARCH PROJECT**

**PN-II-ID-PCE-2011-3-0199**

**Contract nr. 300/05.10.2011**

## **POLYMER MATERIALS WITH SMART PROPERTIES**

**- 2013 -**

*Research Team:*

**CSII Simona Morariu**

**CS I Aurica Chiriac**

**CSII Luminita Ghimici**

**AC Madalina-Luiza Gradinaru**

**AC Cristina-Eliza Brunchi**

**AC Elena-Livia Bibire**

**Project Leader,**

**CSI Maria Bercea**

# BRIEF REPORT

concerning the results obtained by the project team between 16 December 2012 – 15 December 2013

## **Objective 1: Physical gels based on polymer/clay mixtures in aqueous medium**

*Associated Activities:*

- 1.1. Preparation and investigation of gels based on synthetic polymer/clay mixtures
- 1.2. Preparation and investigation of gels based on natural polymer/clay mixtures

## **Objective 2: Evaluation of specific interactions which determine the formation of the interpolymeric complexes for polymer mixtures in solution**

*Associated Activities:*

- 2.1. Investigation of thermodynamic and viscoelastic properties for aqueous solutions of natural and synthetic polymers
- 2.2. Evaluation of natural polymer/synthetic polymer compatibility in aqueous solutions at 37°C

## **Objective 3: Evaluation of specific interactions which determine the formation of supramolecular structures from copolymers in solution**

*Associated Activity:*

- 3.1. Thermodynamic and rheological studies for copolymers in solution

## **Objective 1: Physical gels based on polymer/clay mixtures in aqueous medium**

In the last few years, much attention has been focused on the development of new organic-inorganic hybrid materials because they synergistically combine the chemical, physical, and biological properties of each component. In 2013, the project team investigated tridimensional networks formed by polymers in the presence of clay.

### *1.1. Preparation and investigation of gels based on synthetic polymer/clay mixtures*

Physical gels having as main components a synthetic polymer [poly(ethylene glycol), PEG, with the molecular weight of  $10^4$  g/mol] and a synthetic (Laponite RD) or a natural (Gelwhite H) clay were prepared and their viscoelastic properties were investigated. The two types of clay dispersions (samples denoted L5 and G5) present gel-like properties ( $G' > G''$ ), whereas the aqueous solution 1% PEG (sample PEG1) behaves as a Maxwellian fluid:  $G' \sim \omega^2$  and  $G'' \sim \omega$ . According to the phase diagram presented in literature [Ruzicka et al. *Langmuir* 22, 1106, 2006], aqueous dispersions of smectic clays at low ionic strength and room temperature are in a so-called "repulsive glass" state, when long-distance electrostatic repulsion between the clay particles are dominant. The different behaviors observed for L5 and G5 samples could be explained by the smaller size of Laponite RD particles and therefore the greater number of particles in aqueous L5 dispersion at the same concentration as for the Gelwhite H dispersion.

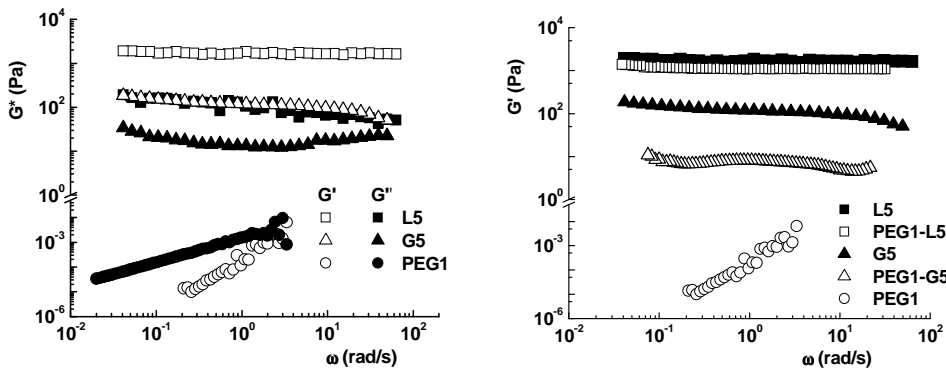
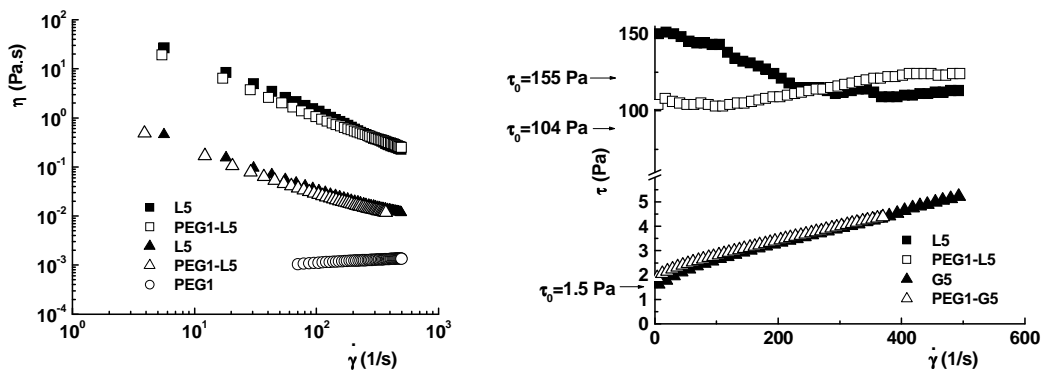


**Figure 1.** The viscoelastic moduli in frequency sweep tests for clay dispersions, polymer solution and polymer/clay mixtures at 20°C.

For PEG/clay hydrogels, the continuous shear experiments revealed a pseudoplastic behaviour characterized by a decrease of the apparent viscosity with increasing the shear rate up to  $500 \text{ s}^{-1}$ . The yield stress ( $\tau_0$ ) was also determined and its value depends on dispersion composition: in the absence of the polymer,  $\tau_0$  is 155 Pa and 1.5 Pa, for Laponite RD and Gelwhite H gels, respectively. The addition of polymer determines the change of the yield stress in different ways for the two types of clays. For Laponite RD gel, a decrease of yield stress from 155 Pa to 104 Pa was observed, the presence of polymer determines the decrease of the interactions between the Laponite particles. For the gels containing Gelwhite H, the polymer addition has no significant influence on  $\tau_0$  value (Figure 2).



**Figur2 2.** Flow curves for clay hydrogels in the presence/absence of PEG.

### 1.2. Preparation and investigation of gels based on natural polymer/clay mixtures

The possibility to modify the rheological properties of hydrogels based on LaponiteRD/PEG by adding small amounts of chitosan (CS) was investigated. PEG sample of 400 g/mol and CS sample of  $7,14 \times 10^5$  g/mol were used. The clay acts as a physical crosslinker and the natural polymer (chitosan) improves the mechanical properties of hydrogels and confers biological properties. For the investigated mixtures we selected constant concentrations of Laponite RD (2.8%) and PEG (2.8%) and samples with different concentrations of CS (shown by the index added to their abbreviation) were prepared (Table 1).

**Table 1.** Samples composition, Newtonian viscosity ( $\eta_o$ ) and yield stress ( $\tau_o$ ) for L/PEG/CS systems

Sample cod	Composition				$\eta_o \times 10^{-3}$ (37°C) (Pa·s)	$\tau_o$ (37°C) (Pa)
	L	PEG	CS	water		
	(%)	(%)	(%)	(%)		
L/PEG	2.8	2.8	0	94.400	0.0473	0.26
L/PEG/CS-0.007	2.8	2.8	0.007	94.393	14.40	24.90
L/PEG/CS-0.096	2.8	2.8	0.096	94.304	26.80	43.00
L/PEG/CS-0.146	2.8	2.8	0.146	94.254	29.57	47.60
L/PEG/CS-0.266	2.8	2.8	0.266	94.134	98.10	73.50
L/PEG/CS-0.453	2.8	2.8	0.453	93.947	131.90	113.00

Oscillatory shear measurements were performed to get information on changes in viscoelastic parameters of L/PEG hydrogels by CS incorporation. Figure 3 presents the variation of the viscoelastic moduli on CS concentration ( $c_{CS}$ ) revealing linear dependences:  $G' = 4898 \cdot c_{CS} + 874$  and  $G'' = 440 \cdot c_{CS} + 40$ . With increasing  $c_{CS}$ , the  $G'$  increase is more pronounced as compared with  $G''$ .

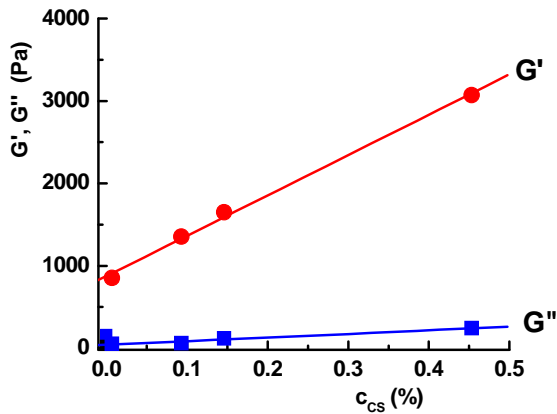


**Figure 3.** Storage ( $G'$ ) ( $\circ$ ) and loss ( $G''$ ) ( $\square$ ) moduli as a function of CS content of the gels at 37°C.

Full symbols, ( $\bullet$ ) and ( $\blacksquare$ ), represent  $G'$  and  $G''$  for L/PEG gel in the absence of CS.

[Morariu et al., *Ind Eng Chem Res* 53(35), 13690-13698, 2014]

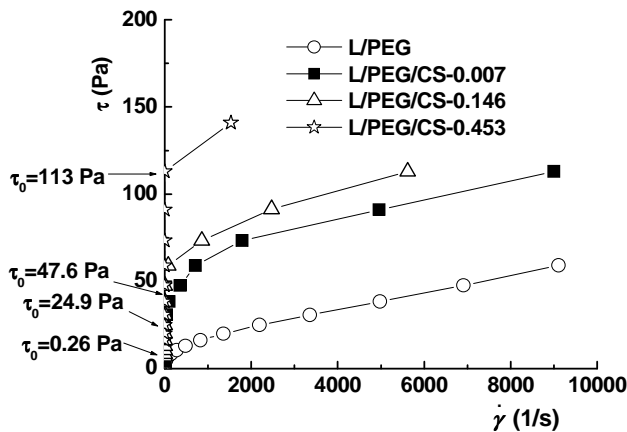


**Figure 4.** Flow curves for pentru L/PEG hydrogels in the presence or absence of CS at 37°C.

The addition of CS into L/PEO hydrogel causes an increase of the viscoelastic parameters due to the formation of a network in which the LRD particles act as cross-linkers between CS chains.

The continuous shear tests have depicted the Newtonian viscosity and pseudoplastic behaviour of the investigated samples above a critical value of the shear rate which shifts to higher values as the chitosan concentration decreases (Table 1). The yields stress value is very low for L/PEO sample (close to zero) and (Figure 4 and Table 1) present a linear increase with  $c_{CS}$  according to:  $\tau_o = 197.5 \cdot c_{CS} + 22.2$ , for  $0.007\% < c_{CS} < 0.453\%$ .

The creep and recovery tests give information about the structural properties of the samples submitted to a constant stress a given period of time followed by recovery after removing the external stress action. Generally, the creep-recovery curve shows the variation of compliance ( $J$ ) as a function of time. The compliance expresses the ratio between the applied stress and total strain at a given time. In the linear viscoelastic range, the compliance can be divided into three components: (1) the instantaneous elastic component ( $J_o$ ); (2) the delayed elastic component ( $J_d$ ); (3) the viscous component,  $J_\infty$ , which is defined as:  $J_\infty = J_{max} - (J_o + J_d)$ , where  $J_{max}$  corresponds to the maximum deformation at the longest time in creep test. The creep-recovery behaviors of the hydrogels with different content of CS are shown in Figure 5. Creep and recovery compliance ( $J$ ) is related with the sample softness. Thus, the higher  $J$  value indicates a weaker material structure and a lower  $J$  value represents a stronger material structure.

Some bonds are irreversibly broken during the creep and the initial structure is not completely recovered. The degree of total elastic recovery ( $R$ ) can be evaluated with the following relationship:

$$R = [(J_{max} - J_\infty) / J_{max}] \times 100 \quad (1)$$

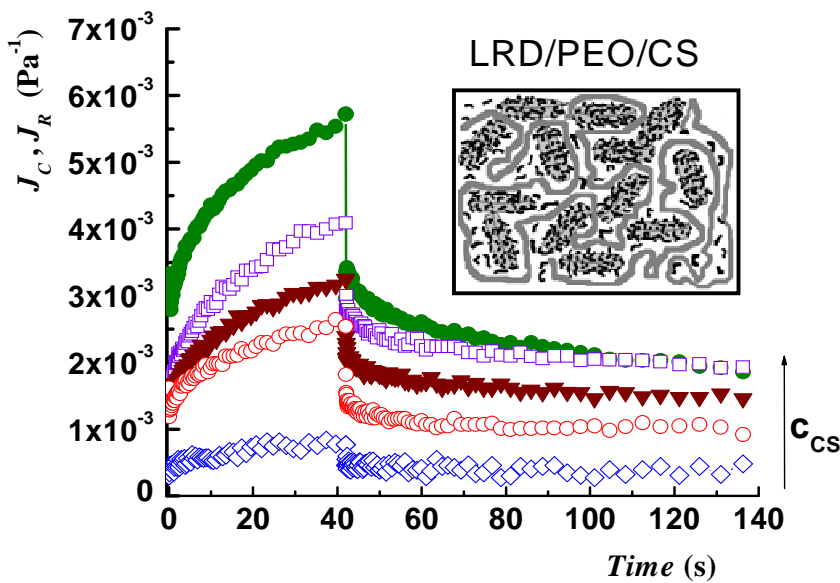


**Figure 5.** Creep and recovery curves for L/PEG hydrogels with different chitosan content [Morariu et al., *Ind Eng Chem Res* 53(35), 13690-13698, 2014]

The creep compliances,  $J_C$ , were evaluated by applying a constant stress of 5 Pa for 40 s and after this period the shear stress was set to zero and the recovery compliances,  $J_R$ , were measured.  $J_{max}$  is

$5.7 \times 10^{-3} \text{ Pa}^{-1}$  for the hydrogel with 0.007% CS and reaches a value of  $7.6 \times 10^{-4} \text{ Pa}^{-1}$  for the hydrogel with 0.453% CS. The decrease of  $J$  by increasing the CS concentration suggests that the gel structure becomes stronger when CS is added into mixture due to the intensification of interactions between clay platelets and polymer chains.

The compliance during recovery process is given by:

$$J = J_{\infty} + J_{KV} \exp(-Bt^m) \quad (2)$$

where  $B$  and  $m$  are parameters which define the recovery rate of system,  $J_{KV}$  is the maximum compliance of Kelvin-Voigt element and  $t$  is the time.

The instantaneous elastic component,  $J_o$ , was determined by using the equation:

$$J_o = J_{max} - (J_{\infty} + J_{KV}) \quad (3)$$

The compliance values and the elastic recovery percentage ( $R$ ) are shown in Table 2.

As can be seen in Table 2 and Figure 6, the recovery degree of hybrid materials decreases by increasing the CS content following a linear relationship:  $R = 69.6 - 54 \cdot C_{CS}$ .

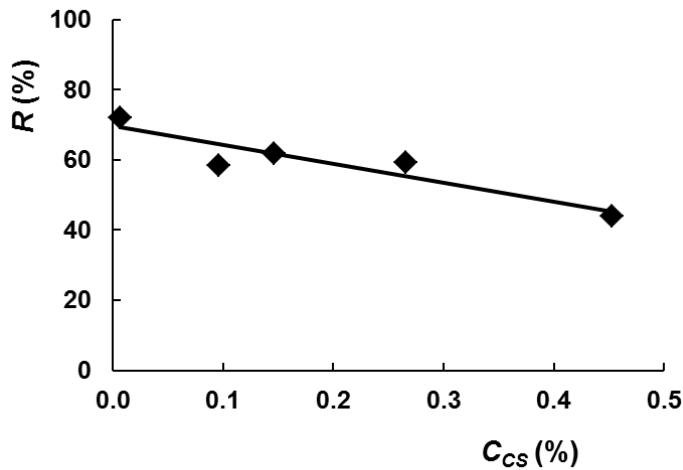


**Figure 6.** The degree of total elastic recovery as a function of CS content at 37 °C. [Morariu et al., *Ind Eng Chem Res* 53(35), 13690-13698, 2014]

**Table 2.** The compliance values and elastic recovery degree of the L/PEG/CS hybrid materials with different content of CS [Morariu et al., *Ind Eng Chem Res* 53(35), 13690-13698, 2014]

Samples	$J_{max} \times 10^3$ ( $\text{Pa}^{-1}$ )	$J_{\infty} \times 10^3$ ( $\text{Pa}^{-1}$ )	$J_d \times 10^3$ ( $\text{Pa}^{-1}$ )	$J_o \times 10^3$ ( $\text{Pa}^{-1}$ )	$R$ (%)
L/PEG/CS-0.007 (cycle 1)	5.70	1.60	1.80	2.30	72.10
L/PEG/CS-0.007 (cycle 2)	3.60	0.60	1.50	1.50	83.90
L/PEG/CS-0.007 (cycle 3)	3.00	0.10	1.50	1.40	96.70
L/PEG/CS-0.096	4.10	1.70	1.20	1.20	58.54
L/PEG/CS-0.146	3.30	1.24	1.06	1.00	61.85
L/PEG/CS-0.266	2.50	1.02	0.48	0.90	59.20
L/PEG/CS-0.453	0.76	0.43	0.03	0.30	45.30

## **Objective 2. Evaluation of specific interactions which determine the formation of the interpolymeric complexes for polymer mixtures in solution**

Thermodynamic properties of solutions of polymers in polar solvents are influenced by the characteristics of macromolecular chains (chemical structure of monomer unit, macromolecular chain length, etc.) and environmental factors (pH, temperature, nature and concentration of salt, dielectric constant, etc.). Hydrodynamic behavior of polymers in solution provides information concerning the size and shape of isolated macromolecules in solution, polymer-polymer interactions, the effect of excluded volume interactions governing the polymer-solvent and chain rigidity. Very often, the behavior of polymers in a given solvent is evaluated through intrinsic viscosity,  $[\eta]$ , a thermodynamic parameter containing information about the conformation of macromolecular chains in solution as well as concerning the polymer-solvent interactions.

### *2.1. Investigation of thermodynamic and viscoelastic properties for aqueous solutions of natural and synthetic polymers*

Usually, the intrinsic viscosity is evaluated by extrapolation of experimental data to zero polymer concentration. Despite a considerable number of theoretical and experimental studies, the current understanding of the viscometric behaviour of polyelectrolyte and even neutral polymer solutions at low concentrations is still far from being complete. Systematic errors appear in the evaluation of the intrinsic viscosity, mainly due to improper technique applied to study the rheological behaviour of polymer solutions at very low concentrations. In this step, we investigated several natural and synthetic polymers in dilute aqueous solutions. Xanthan and poly(vinyl alcohol) (PVA) results obtained in dilute solution were chosen as examples here.

Xanthan aqueous solutions with different content of acetic acid were studied by viscometry and the experimental data were interpreted by using the following equations:

$$\text{Huggins: } \frac{\eta_{sp}}{c} = [\eta]_H + k_H \cdot [\eta]_H^2 \cdot c \quad (4)$$

$$\text{Wolf: } \ln \eta_r = \frac{c[\eta]_W + Bc^2[\eta]_W[\eta]^{\bullet}}{1 + Bc[\eta]_W} \quad (5)$$

$\eta_{sp}/c$  = reduced viscosity;  $c$  = concentration of polymer mixture;  $[\eta]$  = intrinsic viscosity;  $\eta_r$  = relative viscosity;  $k_H$  and  $B$  = hydrodynamic interaction parameters;  $[\eta]^{\bullet}$  = characteristic specific hydrodynamic volume.

The addition of acetic acid, even low concentration, determines a strong decrease of the viscosity as can be observed in the example given in Figure 7. Wolf model [B. A. Wolf, *Macromol. Rapid Commun.*, **28**, 164–170, 2007] is able to describe the viscometric behaviour of polysaccharides in solution of different ionic

strengths, as we have also seen previously for chitosan solutions [Morariu S., Brunchi C.-E., Bercea M., The behaviour of chitosan in solvents with different ionic strengths, *Ind. Eng. Chem. Res.* **51(39)**, 12959-12966, 2012].

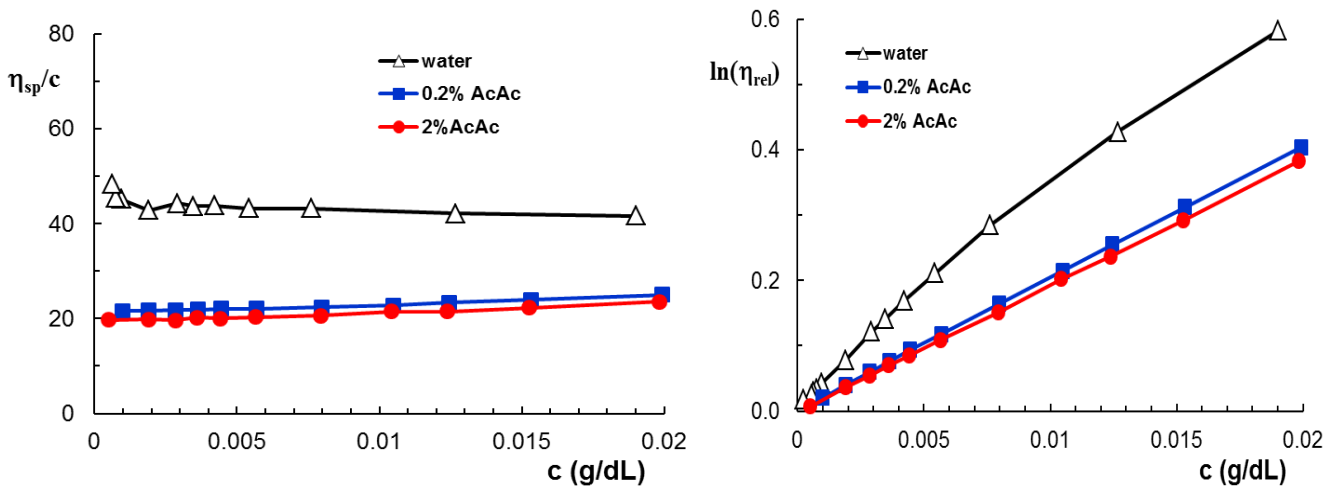


**Figure 7.** Representation of viscometric results obtained for xanthan solutions according to Huggins (eq. (4)) and Wolf (eq. (5)) models.

The aqueous solutions of the samples PVA1 – PVA3 (Table 3) show reduced viscosity plots with maxima in the range of extremely low concentrations (Figure 8). For higher molecular weight samples (PVA4 and PVA5), an upward change in the slope of  $\eta_{sp}/c$  vs.  $c$  dependence was depicted. We also applied the new Wolf approach to calculate the intrinsic viscosity from the initial slope of  $\ln \eta_{rel}$  plots vs. polymer concentration, at sufficiently low shear rates and polymer concentrations.

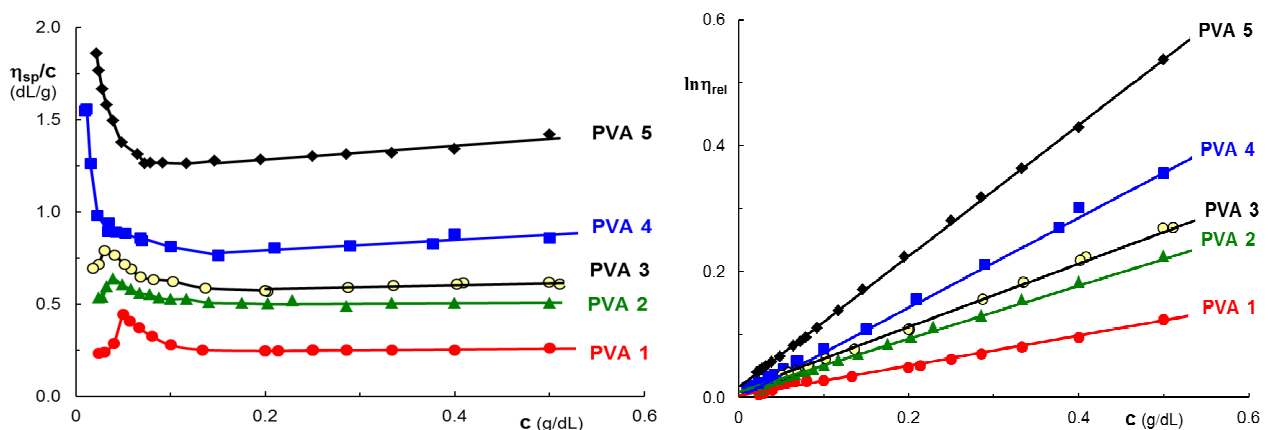


**Figure 8.** Representation of viscometric results obtained for PVA aqueous solutions according to Huggins (eq. (4)) and Wolf (eq. (5)) models.

Figure 9 illustrates a more general picture for PVA aqueous solutions from the dependence of the specific viscosity as a function of a dimensionless parameter,  $c \times [\eta]$ , called coil overlap parameter, which provides an index of the total volume occupied by the polymer. For  $c \leq 1\%$   $\eta_{sp}$  was determined



by capillary viscometry, while for  $c > 1 \text{ g}\cdot\text{dL}^{-1}$   $\eta_{sp}$  was obtained from rheological measurements as shown in Figure 10. Two linear dependences can be seen in a double logarithmic plot  $\eta_{sp}$  vs.  $c \times [\eta]$ , delimiting the critical value  $(c \times [\eta])_{cr}$  of 2.05, from which the overlap concentration,  $c_{cr}$ , can be estimated for PVA samples (see Table 3). The critical concentration,  $c_{cr}$ , delimits two different states of PVA solutions: *isolated macromolecules in solution* (non-entangled state), where  $\eta_{sp} \propto (c \cdot [\eta])$ , and *entangled macromolecules in solution* (entangled state) for which  $\eta_{sp} \propto (c \cdot [\eta])^{3.5}$  [Bercea M., Morariu S., Rusu D., *Soft Matter*, **9**, 1244-1253, 2013].

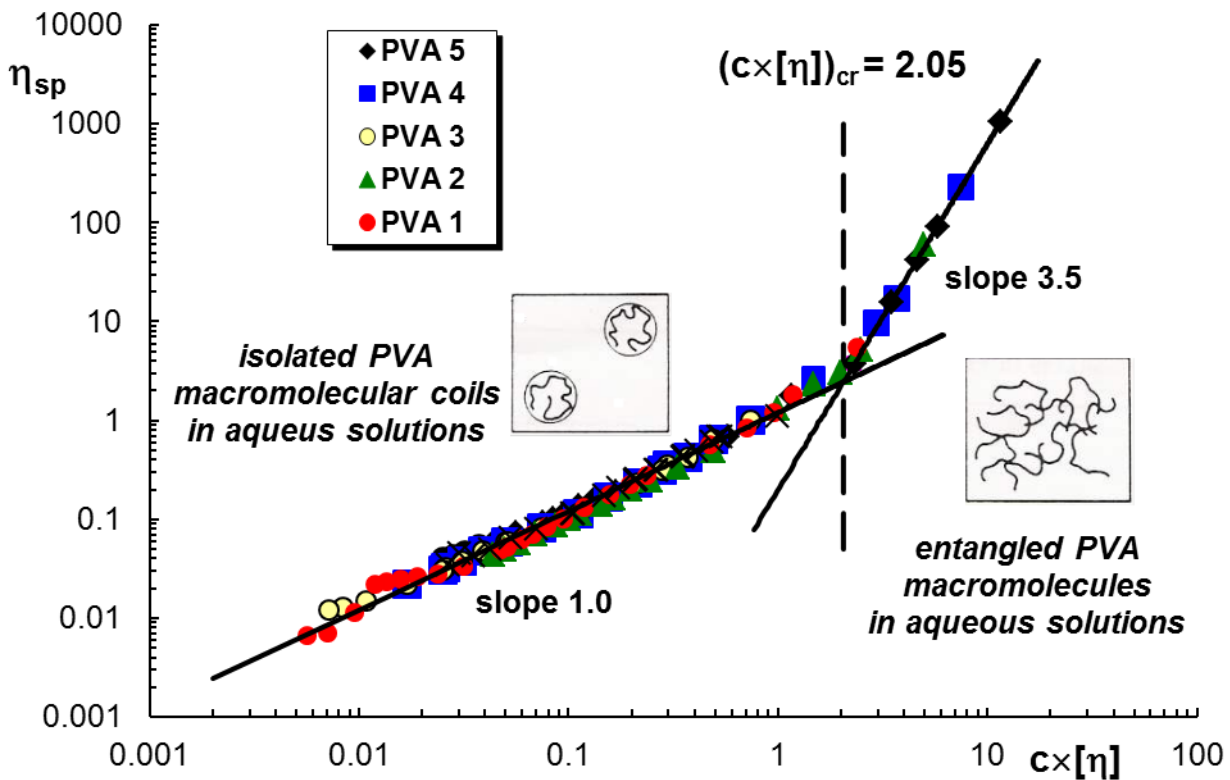


**Figure 9.** Specific viscosity as a function of overlap parameter,  $c \cdot [\eta]$ , for PVA aqueous solutions [Bercea M., Morariu S., Rusu D., *Soft Matter*, **9**, 1244-1253, 2013].

$c_{cr}$  represents the concentration at which the polymer coils touch one another. For  $c > c_{cr}$  intermolecular entanglements predominate on the overall dynamics of polymer chains, and for  $c < c_{overlap}$  the individual macromolecular coils are isolated and free to move independently in the solvent.

**Table 3.** Molecular weights (M), degree of hydrolysis (DH) for PVA samples, and critical concentrations in aqueous solutions

Sample	$M \times 10^{-3}$ (g/mol)	DH (%)	$c_{cr}$ (g/dL)
PVA1	9,5	80	8,72
PVA2	40,5	98-99	4,12
PVA3	65,0	98-99	3,46
PVA4	84,9	98-99	2,61
PVA5	166,0	98-99	1,73

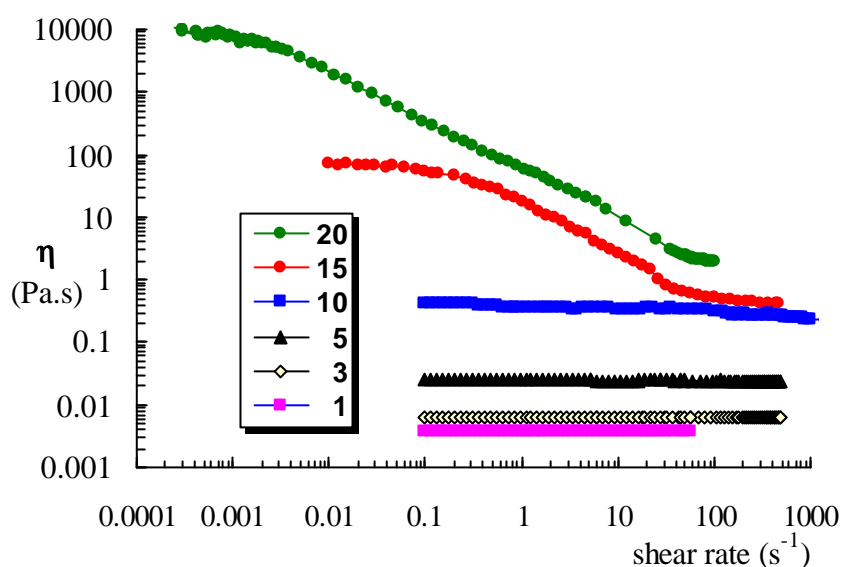


**Figure 10.** Flow curves for aqueous solutions of different concentrations of PVA3 ( $c_{cr} = 3.46$  g/dL) [Bercea M., Morariu S., Rusu D., *Soft Matter*, **9**, 1244-1253, 2013].

The viscosity curves for PVA solutions with  $c < c_{cr}$  (for PVA3 taken as example,  $c_{cr} = 3.46$  g/dL) exhibits Newtonian behaviour over the entire range of shear rates ( $\dot{\gamma}$ ) under study, from  $2 \times 10^{-4} \text{ s}^{-1}$  to  $10^3 \text{ s}^{-1}$  (Figure 10). The transition from Newtonian to non-Newtonian behaviour was observed at shear rates higher than  $1 \text{ s}^{-1}$  for 5 g/dL or  $0.3 \text{ s}^{-1}$  for 10 g/dL, while for 15 g/dL the non-Newtonian flows occurred for  $\dot{\gamma} > 0.03 \text{ s}^{-1}$ . The concentration dependence of the viscosity is stronger for lower shear rates. The range of applied shear rates allowed covering the end of the first Newtonian plateau (low  $\dot{\gamma}$  values) and the beginning of the second one (high shear rates region) [Bercea M., Morariu S., Rusu D., *Soft Matter*, **9**, 1244-1253, 2013]. For all PVA samples, the viscosity plateau corresponding to high  $\dot{\gamma}$  exceeded the solvent viscosity ( $0.798 \times 10^{-3} \text{ Pa}\cdot\text{s}$ ).

## 2.2. Evaluation of natural polymer/synthetic polymer compatibility in aqueous solutions at 37 °C

The compatibility between chitosan (CH) and poly(vinyl alcohol) (PVA) was investigated by viscometry which is frequently used to characterize the interactions between two different polymers in a common solvent. According to this criterion, CH/PVA mixtures are miscible only for  $w_{PVA} > 0.75$  in 0.2% AcAc and fully miscible in 2% AcAc solutions (Figure 11).

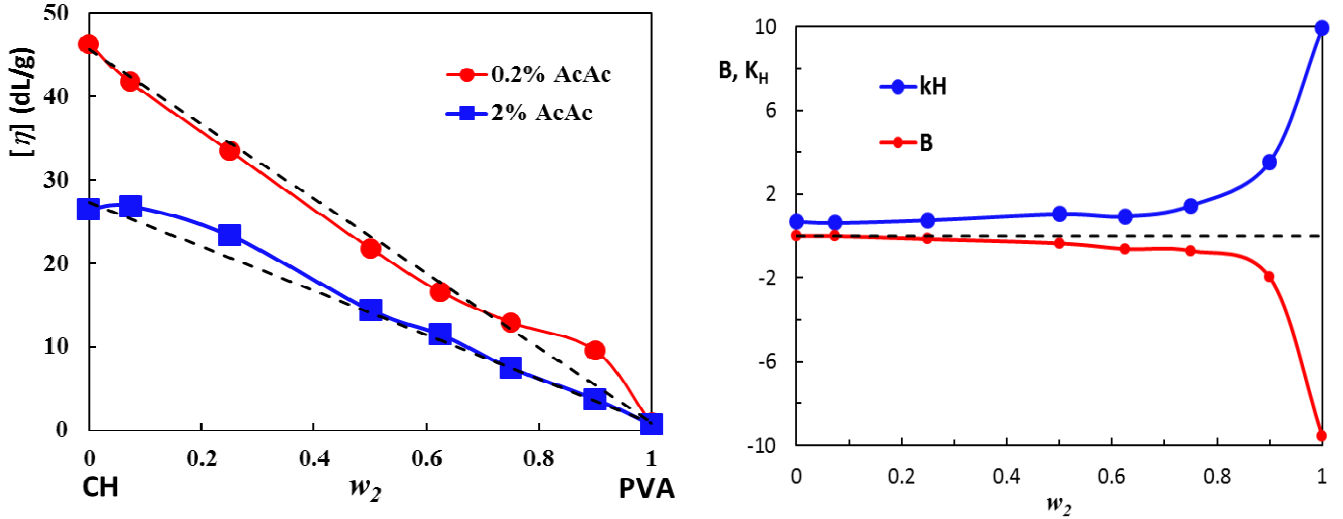


**Figure 11.** (a) Variation of intrinsic viscosity (determined by Wolf method) as a function of polymer mixture composition for CS/PVA mixtures in 0.2% and 2% AcAc at 37 °C; (b) The dependence of hydrodynamic interaction parameters from eqs. (4) and (5) on polymer mixture composition for CS/PVA mixtures in 2% AcAc at 37°C [Morariu et al., *Polym. Bull.* 2014]

Krigbaum and Wall [*J. Polym. Sci.* 5, 505–514, 1950] have proposed the following form for the classical Huggins equation that can be applied to polymer mixtures in a common solvent:

$$\eta_{spm} = [\eta]_m \cdot c_m + b_m \cdot c_m^2 \quad (6)$$

where  $\eta_{spm}$  is the specific viscosity of a polymer mixture in solution,  $[\eta]_m$  is the intrinsic viscosity of the polymer mixture and  $c_m$  represents the total concentration of polymer in solution,  $b_m$  ( $b_m = k_m \cdot [\eta]_m^2$  where  $k_m$  is the Huggins coefficient of the polymer mixture in solution) reflects the binary interactions between polymer segments. Krigbaum and Wall have introduced the parameter  $\Delta b$  defined as:

$$\Delta b = b_{12}^{exp} - b_{12}^{id} \quad (7)$$

$b_{12}$  is a parameter that reflects the interactions between different polymer molecules.

Thus, two polymers are considered compatible if  $\Delta b > 0$  (attractive interactions) and incompatible for  $\Delta b < 0$  (immiscibility or phase separation). For our systems,  $\Delta b \geq 0$  for all polymer compositions in 0.2% AcAc solutions (Figure 12), in agreement with the observations resulted from Figure 11.

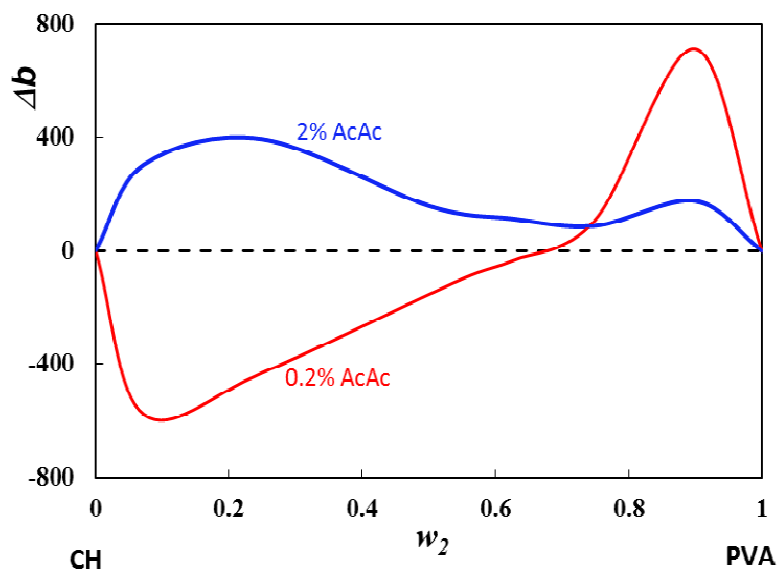


**Figure 12.** Plots of  $\Delta b$  vs. weight fraction of PVA in the CH/PVA binary mixture in AcAc solutions [Morariu et al., *Polym. Bull.* 2014].

These conclusions will be very useful for the next step (in 2014) for designing hybrid materials based on CH/PVA mixtures in the presence of clay.

**Objective 3: Evaluation of specific interactions which determine the formation of supramolecular structures from copolymers in solution**

*3.1. Thermodynamic and rheological studies for copolymers in solution*

Another direction of research in the present project has been designing new hydrogels with potential biomedical applications. The synthesis of new polyurethane was carried out by one member of the team (M.L. Gradinaru) and thermoreversible hydrogels were then elaborated and investigated. A priority in these studies was to obtain biocompatible hydrogels based on natural products and to decrease the amount of toxic products after decomposition of materials. Macromolecular structures able to exhibit rapid and reversible changes of their properties as a result of phase transition phenomena are known as polymer systems with "smart properties". These changes occur under the action of an external stimulus (temperature, pH, electric field, magnetic field, etc.) and are visible at the macroscopic level by increasing turbidity and formation of precipitates or opaque hydrogels.

The formation of thermoreversible gels, especially those with response at temperature close with those of the human body, is of particular interest for biomedical applications. Following the rheological parameters during the gelling process is one of the most useful methods that give information about the formation of three-dimensional structures and the final characteristics of the gels.

Synthesis of polyurethane structures was performed by mass polymerization using Pluronic copolymers and poly(isopropyl lactate) diol as flexible segment (soft) and different aliphatic

diisocyanates as rigid or hard segments as: L-lysine ethyl ester diisocyanate (LDI), hexamethylene 1,6-diisocyanate (HDI) and isophorone diisocyanate (IPDI).

In this stage, we investigated the rheological properties of the polymers in aqueous medium. The temperature sweep tests allowed the evidence of gel formation induced by temperature through viscoelastic parameters: elastic modulus ( $G'$ ), viscous modulus ( $G''$ ), loss angle tangent ( $\tan \delta = G'' / G'$ ) and complex viscosity ( $\eta^*$ ). In Figure 13 is represented evolution of complex viscosity with temperature for polyurethane structures HDI PU, PU and PU-IPDI-LDI in aqueous systems. Samples were heated slowly, the temperature being controlled by a Peltier system. The heating rate influences the response of the sample to the thermal stimulus. All samples are in sol state at low temperatures (less than 15°C) and the viscosity is less than 0.05 Pa·s. Above 25°C, the viscosity sharply increases more than three orders of magnitude. This increase occurs in a narrow range of temperature - approx. 5°C - and the transition point is influenced by the polymer structure. This sharp increase in viscosity is due to the rapid response of macromolecular structures to thermal stimulus. This phenomenon can be attributed to intermolecular interactions which are weak at low temperatures and determine the formation of micelles or associated micelles.

With increasing the temperature, the interactions between micelles increases the hydrophobic-hydrophilic balance changes, leading to the formation of well-defined crystal structures [Gradinaru et al. *Ind. Eng. Chem. Res.* 51, 12344, 2012]. From Figure 13 it can be seen that after the high increase of the viscosity up to approx. 40°C, a plateau is reached, and then a slow decrease occurs. The transition temperature from the sol state to the gel state and from the gel to the sol for PU-IPDI is smaller than for the PU-PU-HDI and LDI samples. At 37°C, PU-HDI shows a higher viscosity.

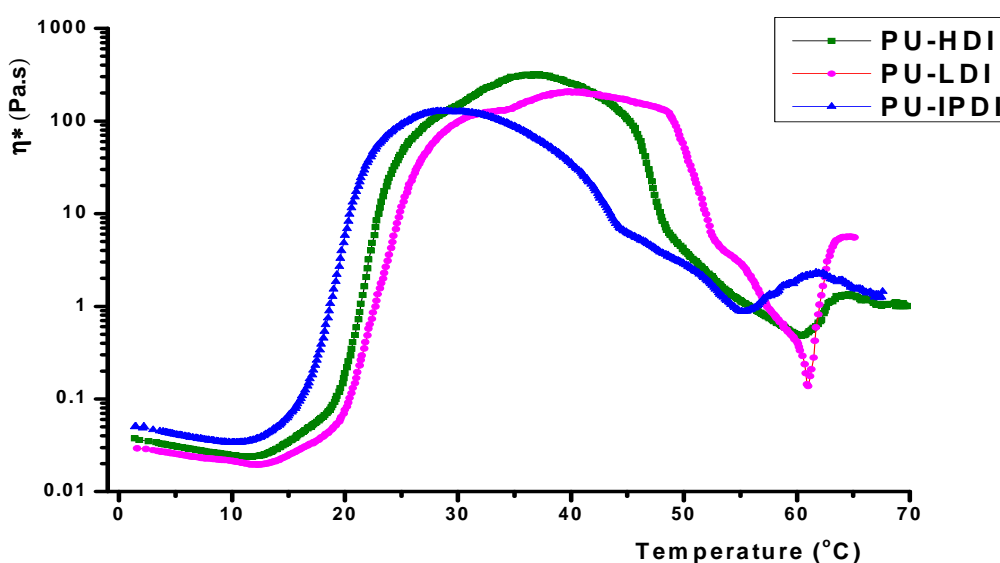


**Figure 13.** Viscosity – temperature dependence for different polyurethane structures in aqueous solutions.

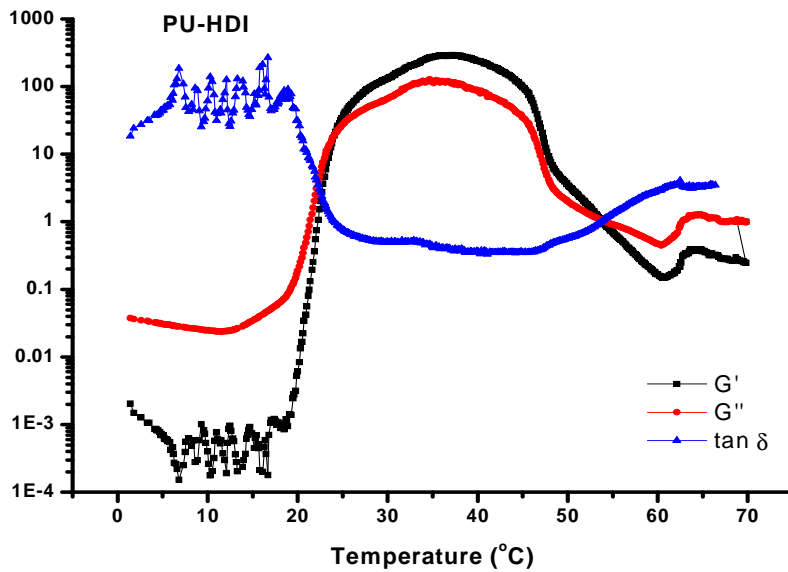


**Figure 14.** Temperature dependence of viscoelastic parameters for PU-HDI sample.

Figure 14 shows the evolution of viscoelastic parameters on the temperature for one sample (PU-HDI). We can observe that the sol state exists at low temperatures when  $G'' > G'$  and  $\tan \delta$  is high, then the gel state is achieved at temperatures close to body temperature and the viscosity decreases over  $50^\circ\text{C}$  when the gel eliminates more than 95% of water content. Near the gel point (approx.  $22^\circ\text{C}$ ), the viscoelastic parameters change suddenly by increasing the temperature and the gel state is quickly reached.  $G'$  grows faster than  $G''$  and its value is about 5 orders of magnitude higher than those registered in the sol state. For PU-LDI sample, the gel state is maintained in a broader range of temperature ( $20^\circ\text{C} - 50^\circ\text{C}$ ) and samples PU-PU-HDI and LDI show maximum value of  $G'$  at  $37^\circ\text{C}$ . In conclusion, under the action of a thermal stimulus, polyurethane structures can undergo sol-gel transition in aqueous medium, when the macromolecular chains are connected into a network structure through physical interactions such as hydrogen bonds, electrostatic attraction, van der Waals forces and hydrophobic interactions. Polyurethane structures with predictable properties can be designed, as for example a structure with the transition temperature close to those of the human body. Thus, the sample is stored in sol state at low temperature and it is introduced into human body when the gel formation can occur during tens of seconds or minutes, important in biomedical applications.

**All objectives were fully realized in this stage and some results were included into manuscripts submitted to publication.**

#### **Results dissemination**

- 7 papers were published in journals indexed by web of knowledge; 1 book was also published.
- The team members participated at 15 scientific events with 4 oral presentations and 11 posters.